

Conduction-electron polarization and moment perturbations in dilute Fe₃Si-based alloys

Mary Beth Stearns

Physics Department, Research Staff, Ford Motor Company, Dearborn, Michigan 48121

(Received 22 July 1977)

The spatial variation of the *s*-conduction-electron polarization in the Fe₃Si system is determined from the measured hyperfine fields of the near-stoichiometric Fe₃Si alloys. This polarization is then combined with the hyperfine-field data from Mn, V, Co, and Ni solutes and used to derive the solute moments and moment perturbations in Fe₃Si to obtain the solute-moment and host-moment perturbations caused by these impurities. The behavior of these solute moments and moment perturbations is seen to be very similar to that of the same solutes in binary Fe alloys. Since Fe₃Si is closely related to Heusler alloys, it is suggested that their magnetic behavior is also governed by the same mechanism that determines the magnetic behavior of binary Fe alloys; that is, the conduction *d*-like electrons, *not s*-like electrons, are responsible for the magnetic alignment.

I. INTRODUCTION

In general, the conduction electrons of transition metals can be considered as two types; *s*-like and *d*_i-like. Thus, a transition-solute atom affects the host atoms in its vicinity through two separate mechanisms. One is due to the change in the *s*-like conduction-electron polarization (*s*-CEP). The other is due to the *d*_i-like conduction electrons, which are also polarized through exchange interactions with the localized *d*_i moments. Although the *s*-conduction-electron polarization is very evident through its contribution to the hyperfine field, it plays no major role in determining the magnetic alignment. This is because the *s*-*d*_i interaction is weak relative to the *d*_i-*d*_i interaction, as manifest by the small degree of *4s*-like polarization and large degree of *d*_i-like polarization in Fe. This *d*_i-like polarization is seen directly in tunneling between a ferromagnet and a superconductor.^{1,2} Since the wave functions of the *d*_i and *d*_i electrons are very similar, the *d*_i polarization is detected as moment changes on the nearby magnetic host atoms. A procedure^{3,4} for distinguishing these two mechanisms was developed for dilute Fe alloys with transition metals and will be applied here to the Fe₃Si system.

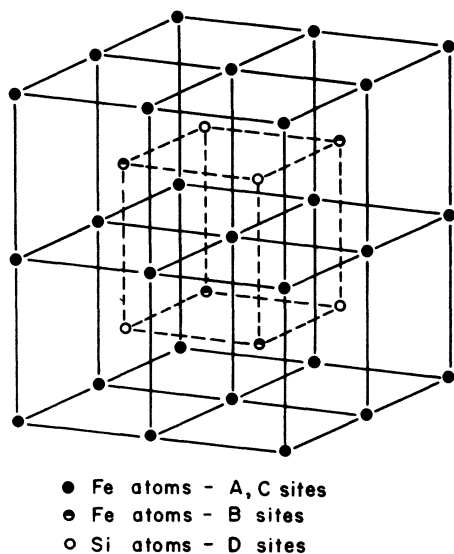
The magnetic behavior of the Fe₃Si system has been studied in great detail.⁵⁻¹¹ It is a particularly interesting system for many reasons. We shall see that its behavior as a host for a variety of transition-metal solute atoms is much like that of dilute binary alloys of Fe. As has been previously discussed^{3,4} the magnetic behavior of the dilute binary alloys is essentially determined by the number of localized and itinerant *d*_i or *d*_i electrons. Table I indicates the variation of *d*_i and *d*_i character of the transition elements. In the

elemental metallic state, the elements to the left of the dashed line have only *d*_i-like electrons, Mn, Fe, Co, and Ni have both *d*_i and *d*_i electrons, while Cu, Ag, and Au have only *d*_i electrons. In alloys, the *d*_i, *d*_i character is intermediate between that of the constituents (principle of accommodation). For elements or alloys with unpaired *d*_i electrons, the *d*_i electrons are polarized through Coulomb exchange and hybridization interactions with the *d*_i electrons. It has been proposed^{3,4,12} that the magnetic behavior is determined by the number of *d*_i-like electrons. The number of *d*_i electrons can be controlled by alloying elements with varying *d*_i and *d*_i character. For binary Fe alloys, densities of about 0.4 or more *d*_i electrons per atom tend to have a *d*_i polarization behavior which leads to antiferromagnetic alignment, while densities of less than about 0.4 electrons per atom produce ferromagnetic coupling. A similar situation appears to exist for alloys with Fe₃Si as the host and also for the large class of "Heusler alloys" with a similar structure. Fe₃Si has a DO₃ structure as shown in Fig. 1. This is a variant of the L2₁ structure of the Heusler alloys X₂YZ, where X corresponds to the A and C sites of Fig. 1, Y to the B sites, and Z to the D sites which are occupied by Si in Fe₃Si. In Heusler alloys Z is usually an *sp* element and Y is a transition metal, most often Mn, but sometimes other transition metals to the left of Fe in the Periodic Table and the X atoms are transition elements to the right of Fe in the Periodic Table. We suggest that the Heusler alloys are similar to the binary alloys in that the magnetic behavior is also determined by the *d*_i electrons, rather than *s*-conduction electrons. This approach is different from all other attempts at explaining the magnetic alignment of Heusler alloys which assume, with some difficulty, that the *s*-conduction electrons

TABLE I. Variation of the character of the d electrons.

		← d_i d_f →									
	Sc	Ti	V	Cr	Mn	Fe	Co	Ni	Cu		
d_i	Y	Zr	Nb	Mo	Tc	Ru	Rh	Pd	Ag		
↓	La	Hf	Ta	W	Re	Os	Ir	Pt	Au		

are mediating the magnetic alignment. As in the case of binary alloys, the magnetic alignment is thus determined by the degree of itinerancy of the d electrons. This is controlled by combining a transition element Y with many d_i electrons, i.e., $3d$ elements to the left of Fe, with another transition element X , which has predominately localized d_f electrons. Thus, the Heusler alloys are materials with the correct combination of d_i and d_f electrons to give rise to a d_i polarization which provides the magnetic coupling. The role of the sp elements may be simply as a dilutant or more likely there appears to be evidence that their covalent hybridization may participate in binding the crystal which attains the proper mixture of d_i and d_f electrons. In a comprehensive series of experiments, Budnick and his co-workers^{7,9-11} have shown that, in a manner similar to the behavior in Heusler alloys, transition elements beneath and to the right of Fe in the Periodic Table tend to go into A and C sites while transition elements to the left of Fe tend to go into B sites. In this paper we will not further be concerned with the similarities of Fe_3Si and the Heusler alloys but to a determination of the s -like conduction electron polarization surrounding a moment in the Fe_3Si host and to the moment perturbations surrounding a solute atom in this host.

FIG. 1. Structure of ordered Fe_3Si .

In earlier papers^{3,4} we developed a procedure, using saturation magnetization and hyperfine-field (hff) shifts to determine the moment perturbations in dilute alloys. We use a similar procedure here, adapted to the Fe_3Si lattice. In Sec. II we use the data of Ref. 8 to determine the hff shifts due to s -CEP and moment perturbations of an Fe atom substituted into a Si D site. This procedure is an improvement of the analysis in Ref. 8 where, for higher than first-nearest-neighbor ($1nn$) shells, we neglected the moment perturbations. In Secs. III and IV we then use these s -CEP values which characterize the Fe_3Si host with magnetization and hff shift data to determine the solute moment and the moment perturbation surrounding dilute alloys in which a $3d$ transition element is substituted into Fe A or Fe B sites. The approximations and their validity are discussed thoroughly in Refs. 3 and 4. We will see that the moments and moment perturbations behave in a very similar fashion to those obtained for the dilute alloys of Fe. For the dilute alloys⁴ we found that the shape of the moment perturbations depended on the difference in number of itinerant d_i -like electrons contributed by the solute atom relative to the number in the host. The moment perturbations are seen to be oscillatory and to decrease with distance from the solute atom, i.e., they have a Ruderman-Kittel-Kasuya-Yosida- (RKKY) like behavior.

II. $\text{Fe}_3^{A,C,B}\text{Fe}_x^D\text{Si}_{1-x}$

Alloys in which an Fe atom has been substituted into a Si D site have been thoroughly studied by many techniques so that at present we can accurately characterize this system. In particular we know the moments, saturation magnetization behavior, and hyperfine fields at the Fe A , Fe B , and Si sites in Fe_3Si as well as many hyperfine-field shifts due to known occupational configurations off stoichiometry. Assuming that the s -CEP contributions and moment perturbations are additive for small concentrations of Fe atoms on Si D sites, we will see that we can obtain the hff s -CEP contributions and moment perturbations for the first four neighbor shells surrounding an Fe atom substituted into a Si D site. Although the $4nn$ contributions are small, we will keep them because there are 24 atoms in this shell and their accumulative effect might be considerable.

A. Moment evaluations

Neutron-scattering experiments⁶ have shown that the Si atoms have essentially no moment, as expected. The ratio of μ_B/μ_A was found to be 2.0. Saturation magnetization measurements¹¹ at 6.5°K give a moment of $4.82 \mu_0$ per Fe_3Si molecule in Fe_3Si and a slope $d\bar{\mu}/dx = 3.66 \mu_0$ per Fe atom in a Si D site or removed from a Fe B site, where μ_0 is the Bohr

TABLE II. Quantities used in the analysis of $\text{Fe}_3\text{Fe}_x\text{Si}_{1-x}$ (all moments in μ_0 and hff values in kG).

Quantity	Value
μ_B/μ_A	2.0
$\bar{\mu}$ (per Fe_3Si molecule)	4.82
μ_{Si}	0
μ_A	1.21
μ_B	2.40
$d\bar{\mu}/dx$ (per Fe D atom)	3.66
H_B^0	-342
H_A^0	-222
H_{Si}^0	-41 or +33
ΔH_A	-52.3
ΔH_B^2	-7.5
ΔH_{Si}^3	(\pm)2.5 \pm 1
ΔH_A^4	+4.2

magneton. For $\mu_{\text{Si}}=0$ this gives $\mu_A=1.21\mu_0$ and $\mu_B=2.4\mu_0$. All these values are listed in Table II. The slope of the magnetization curve is simply related to the moment perturbations surrounding an Fe D atom by³

$$\frac{d\bar{\mu}}{dx} = \mu_D + \sum M_n \Delta_n = \mu_D + 8\Delta_1 + 6\Delta_2 + 24\Delta_4, \quad (1)$$

where M_n is the number of sites in the n th shell surrounding the Fe D solute atom and Δ_n is the moment perturbation in the n th shell surrounding the Fe D solute atom. In Table III we list the number and type of neighbors through the fourth-nearest-neighbor (4nn) shell for the various sites in Fe_3Si .

B. Hyperfine fields in Fe_3Si

We use the following model^{8,12,13} to describe the hff. The hff is considered to be composed of three parts

$$H_z = H_{\text{cp}}^z + H_{\text{ce}} + H_v. \quad (2)$$

We have assumed no orbital contributions. H_{cp}^z is due to the polarization of the core s electrons; for $3d$ transition atoms there are $1s$, $2s$, and $3s$ electrons. This contribution only occurs for atoms that have a

moment. H_{ce} is due to the s -like conduction electrons; for $3d$ atoms these are $4s$ electrons. H_v is positive volume misfit term which is due to overlap,¹⁴ covalency, and lattice distortion terms which exist when a solute atom is larger than a given volume available to it in a host lattice. Since transition-metal atoms have small atomic volumes, this term is generally zero for transition-metal solutes. In the Fe_3Si system only the hff at Si could have an H_v term; its atomic volume is 12.0 compared to that of 7.1 for Fe.

Another hff model has been proposed¹⁵ to describe the hff at nonmagnetic sp -solute atoms. The main difference of this model from that given above when applied to a nonmagnetic solute is that the solute atom is considered to cause a strong charge perturbation and thus the s -CEP part of the hff is not considered to be separable as assumed in Eq. (2). There seems to be a large amount of evidence¹³ that the H_v term is separable, so we will assume that it is here.

In using the hff model described by Eq. (2) it is convenient to let $H_{\text{ce}} = H_s + H_{\Sigma}$ where H_s is the conduction-electron contribution coming from the atom whose hff we are considering, i.e., the self-polarization of the $4s$ electrons by the atom itself. H_{Σ} is the hff contribution from the s -CEP of all the surrounding atoms and is given by

$$H_{\Sigma}^{\text{Fe}} = \sum_n M_n h_n \mu_n,$$

where h_n is the hff at an Fe atom due to an atom with a moment of one μ_0 in the n th shell. M_n is the number of atoms in the n th shell and μ_n is the moment in Bohr magnetons μ_0 of the atoms in the n th shell. Then for transition metal atoms we have

$$H_z = H_M^z \mu_z + \sum \frac{M_n h_n \mu_n A_z}{A_{\text{Fe}}}, \quad (3)$$

where $H_M^z = H_{\text{cp}}^z + H_s$ is the hff at an atom due to its own moment and A_z is the hff coupling constant of atom Z . For convenience, we have redefined H_{cp}^z and H_s as fields per μ_0 . A_z is the hyperfine coupling constant which scales the s -like conduction electrons to the nucleus of atom Z , since the h_n 's are defined for Fe.

For dilute alloys and assuming additivity we obtain the following expression from Eq. (3) for the hff value H_A^0 at an Fe A site in stoichiometric Fe_3Si (see Table III):

TABLE III. Number and type of neighbors for the three sites in Fe_3Si . See Fig. 1 for a labeling of the sites.

Type	1nn	2nn	3nn	4nn
Fe A	4 Fe B -4 Si D	6 Fe A	12 Fe A	12 Fe B -12 Si D
Fe B	8 Fe A	6 Si D	12 Fe B	24 Fe A
Si D	8 Fe A	6 Fe B	12 Si D	24 Fe A

$$H_A^0 = H_M^{\text{Fc}} \mu_A + 4h_1 \mu_B + 6h_2 \mu_A + 12h_3 \mu_A + 12h_4 \mu_B \quad (4)$$

This value was measured to be -218 kG.⁸ This must be corrected for the Lorentz term $(\frac{4}{3}\pi)M_s$, which is about -4 kG for Fe_3Si . Thus we have $H_A^0 = -222$ kG as listed in Table II. In Eq. (4) we again have assumed there are no contributions to the hff from orbital momentum. In treating the dilute alloys we have found that this appears to be valid for all the 3d transition elements except Co and Ni. These do seem to have an orbital contribution, which we will consider later.

Similarly, for an Fe *B*-type atom we have (see Table III)

$$H_B^0 = H_M^{\text{Fc}} \mu_B + 8h_1 \mu_A + 12h_3 \mu_B + 24h_4 \mu_A \quad (5)$$

This value has been measured to be $-338 - 4 = -342$ kG.⁸

For the hff at a Si atom we have from Table III:

$$H_{\text{Si}}^0 = (8h_1 \mu_A + 6h_2 \mu_B + 24h_4 \mu_A) A_{\text{Si}/\text{Fe}} + H_V^{\text{Si}} = H_V^0 A_{\text{Si}/\text{Fe}} + H_V^{\text{Si}} \quad (6)$$

H_{Si}^0 was measured to be $|37.3|$ kG.⁸ The sign of the field has not been conclusively determined. If it is

positive, we have $H_{\text{Si}}^0 = 33$ kG; if negative, $H_{\text{Si}}^0 = -41$ kG.

C. Hyperfine fields in $\text{Fe}_3\text{Fe}_x\text{Si}_{1-x}$

We now derive expressions for the hff shifts at atoms which are in various neighbor shells from an Fe *D* solute atom. The procedure is a straightforward consideration of the occupational configurations. In Table IV we list the distribution of atoms surrounding an atom which is the *n*th neighbor to an Fe *D* solute atom.

1. First-nearest-neighbor shift for Fe *A* sites

Group 1 of Table IV lists the type of atoms surrounding an Fe *A* atom which is a 1nn to an Fe *D* atom which has replaced a Si *D* atom. In the first column of Table IV we see that the nearest neighbors to this Fe *A* atom are a (1nn) Fe *D* atom, three second-nearest-neighbor (2nn) Fe *B* atoms, three third-nearest-neighbor (3nn) Si *D* atoms and one fifth-nearest-neighbor (5nn) Fe *B* atom. Any Fe atoms in the *n*th shell surrounding an Fe *D* solute atom will have a moment perturbation of Δ_n . It has been shown that for small concentrations the hff shifts are linear^{5,7,8,10}; thus, it is a good assumption that the moment perturbations are additive. We

TABLE IV. Occupation distribution for various atoms which are *n*th neighbor to an Fe *D* atom.

1nn	Shell with respect to Fe <i>D</i>	2nn	Shell with respect to Fe <i>D</i>	3nn	Shell with respect to Fe <i>D</i>	4nn	Shell with respect to Fe <i>D</i>
Fe <i>A</i> which is 1nn to Fe <i>D</i>							
Fe <i>D</i>	1nn	3 Fe <i>A</i>	1nn	3 Fe <i>A</i>	1nn	3 Fe <i>B</i>	2nn
3 Fe <i>B</i>	2nn	3 Fe <i>A</i>	4nn	6 Fe <i>A</i>	4nn	6 Si <i>D</i>	3nn
3 Si <i>D</i>	3nn			3 Fe <i>A</i>	7nn	9 Fe <i>B</i>	>5nn
1 Fe <i>B</i>	5nn					6 Si <i>D</i>	>6nn
Fe <i>B</i> which is 2nn to Fe <i>D</i> .							
4 Fe <i>A</i>	1nn	Fe <i>D</i>	2nn	4 Fe <i>B</i>	2nn	4 Fe <i>A</i>	1nn
4 Fe <i>A</i>	4nn	4 Si <i>D</i>	3nn	4 Fe <i>B</i>	5nn	8 Fe <i>A</i>	4nn
		1 Si <i>D</i>	6nn	4 Fe <i>B</i>	8nn	12 Fe <i>A</i>	>7nn
Si <i>D</i> which is 3nn to Fe <i>D</i>							
2 Fe <i>A</i>	1nn	2 Fe <i>B</i>	2nn	Fe <i>D</i>	3nn	4 Fe <i>A</i>	1nn
4 Fe <i>A</i>	4nn	2 Fe <i>B</i>	5nn	4 Si <i>D</i>	3nn	6 Fe <i>A</i>	4nn
2 Fe <i>A</i>	7nn	2 Fe <i>B</i>	8nn	7 Si <i>D</i>	>6nn	14 Fe <i>A</i>	>7nn
Fe <i>A</i> which is 4nn to Fe <i>D</i>							
1 Fe <i>B</i>	2nn	1 Fe <i>A</i>	1nn	2 Fe <i>A</i>	1nn	1 Fe <i>D</i>	4nn
2 Si <i>D</i>	3nn	2 Fe <i>A</i>	4nn	3 Fe <i>A</i>	4nn	2 Fe <i>B</i>	2nn
3 Fe <i>B</i>	>5nn	3 Fe <i>A</i>	>7nn	7 Fe <i>A</i>	>7nn	3 Si <i>D</i>	3nn
2 Si <i>D</i>	>6nn					18 Fe <i>B</i>	>5nn

further assume that the same Δ_n values apply to the Fe *A* and Fe *B* atoms. Since we envisage that the Δ_n 's are due to the difference in number of *d*, electrons, this implies that the band structure of each type Fe atom is similar enough that the number of *d*-like electrons associated with each type Fe is about the same. This may not be true, but we assume any deviations are small. We shall further assume the $\mu_D = \mu_B$ which is what would result from the moment being determined mainly by the 1nn. Thus, using Table IV we can write an expression for the hff at an Fe *A* site which is a 1nn to an Fe *D* atom

$$\begin{aligned} H_A^1 = & H_M^{\text{Fe}}(\mu_A + \Delta_1) + h_1(\mu_D + \mu_B) + 3h_1(\mu_B + \Delta_2) \\ & + 3h_2(\mu_A + \Delta_1) + 3h_2(\mu_A + \Delta_4) + 3h_3(\mu_A + \Delta_1) \\ & + 6h_3(\mu_A + \Delta_4) + 3h_3\mu_A + 3h_4(\mu_B + \Delta_2) + 9h_4\mu_B . \end{aligned}$$

Defining the shift $\Delta H_A^1 + H_A^1 - H_A^0$, we have

$$\begin{aligned} \Delta H_A^1 = & H_M^{\text{Fe}}\Delta_1 + h_1\mu_D + 3h_1\Delta_2 + 3h_2\Delta_1 + 3h_2\Delta_4 \\ & + 3h_3\Delta_1 + 6h_3\Delta_4 + 3h_4\Delta_2 . \end{aligned} \quad (7)$$

ΔH_A^1 was measured to be -52.3 kG.⁸

Note that Eq. (7) can be quite simply written directly from Table VI, the first term being the contribution from the moment increase on Fe *A* due to being a 1nn to Fe *D*, the second being due to the *s*-CEP contribution from the Fe *D* atom, and the rest also being *s*-CEP contributions written sequentially for all the moment changes of the atoms in the first group in Table IV. From now on we shall directly write the shifts from Table IV. Since the hff shifts are the difference of two hff values, any orbital contributions would cancel out, so in that sense they give more accurate information than the hff values.

2. Second-nearest-neighbor shift for Fe *B* sites

The hff shift for Fe *B* atoms which are 2nn to an Fe *D* atom is seen from the second group of Table IV to be $\Delta H_B^2 = H_B^2 - H_B^0$,

$$\begin{aligned} \Delta H_B^2 = & H_M^{\text{Fe}}\Delta_2 + h_2\mu_D + 4h_1\Delta_1 + 4h_1\Delta_4 + 4h_3\Delta_2 \\ & + 4h_4\Delta_1 + 8h_4\Delta_4 . \end{aligned} \quad (8)$$

ΔH_B^2 was measured to be -7.5 kG,¹⁶ as listed in Table II.

3. Third-nearest-neighbor shift for Si *D* sites

We use Eq. (3) to evaluate the hff at Si. The Si atoms are 3nn to an Fe *D* atom. From Table IV we see that the hff shift $\Delta H_{Si}^3 = H_{Si}^3 - H_{Si}^0$ is given by

$$\begin{aligned} \Delta H_{Si}^3 = & (h_3\mu_D + 2h_1\Delta_1 + 4h_1\Delta_4 + 2h_2\Delta_2 \\ & + 4h_4\Delta_1 + 6h_4\Delta_4) A_{Si}/A_{Fe} \\ = & H_{Si}^3 A_{Si}/A_{Fe} , \end{aligned} \quad (9)$$

where H_{Si}^3 would be equivalent *s*-CEP contribution at an Fe nucleus.

We have made the reasonable assumption that the H_V term is the same for a Si *D* atom whether or not it has a 3nn Fe *D* atom. The analysis to determine ΔH_{Si}^3 is the most evolved in Ref. 8 and therefore this quantity is least accurately known. ΔH_{Si}^3 was measured to be $|2.5 \pm 1|$ kG. It is $+2.5$ kG if H_{Si}^0 is negative and -2.5 kG if H_{Si}^0 is positive.

4. Fourth-nearest-neighbor shift for Fe *A* sites

The Fe *A* atoms which are 4nn to Fe *D* atoms are seen from Table IV to have a hff shift given by $\Delta H_A^4 = H_A^4 - H_A^0$,

$$\begin{aligned} \Delta H_A^4 = & H_M\Delta_4 + h_4\mu_D + h_1\Delta_2 + h_2\Delta_1 + 2h_2\Delta_4 \\ & + 2h_3\Delta_1 + 3h_3\Delta_4 + 2h_4\Delta_2 . \end{aligned} \quad (10)$$

ΔH_A^4 was measured to be $+4.2 \pm 0.5$ kG.⁸ Note that ΔH_A^4 would be zero in a 1nn approximation, where only h_1 and $\Delta_1 \neq 0$. Its existence indicates that there are *s*-CEP contributions and/or moment perturbations as far out as the 4nn shell.

D. Evaluation of h_n 's and Δ_n 's

We can evaluate H_M^{Fe} as follows: Since Cu is a small atom (and also has the same effective charge as Fe) its hff when a solute atom in Fe is entirely due to the *s*-CEP contributions. Thus, its hff value gives H_{Σ} directly by $H_{\Sigma}^{\text{Fe}} = H_{Cu} A_{Fe}/A_{Cu}$. Correcting for the Lorentz field in Fe $-(\frac{4}{3}\pi)M_s = -7$ kG, the hff at Cu was measured to be -220 kG.¹⁷ The hff coupling constants have been estimated by many authors¹⁸⁻²⁰ with an average ratio for A_{Cu}/A_{Fe} being ≈ 1.4 . Thus $H_{\Sigma}^{\text{Fe}} = -155 \pm 10$ kG. A similar value of ≈ -145 G was also obtained by summing the *s*-CEP contributions from the various shells.¹² The value of H_M^{Fe} can then be obtained from the measured hff (-346 kG) at Fe and is $H_M^{\text{Fe}} = H_{Fe} - H_{\Sigma}^{\text{Fe}} = -191$ kG or -86 ± 5 kG/ μ_0 .

Since H_V for H_{Si}^0 is in doubt we temporarily neglect Eqs. (6) and (9). Considering through the 4nn we then have six equations relating seven unknowns, the four h_n values, and three moment perturbations. By examination of the equations, it can be seen that certain quantities are mainly dependent on selected parameters: For example, ΔH_A^1 depends mainly on h_1 and Δ_1 , ΔH_B^2 on h_1 , h_2 , Δ_1 , and Δ_2 , and ΔH_A^4 is determined mainly by h_4 and Δ_4 . The final parameters are quite definitely determined and are listed in Table V. The value of h_1 ($= -12$ kG/ μ_0) is seen to be essentially the same as the value obtained¹² for dilute alloys of Si in Fe. The other h_n values are quite different from those obtained earlier⁸ by neglecting the moment changes in this system and assuming that the measured shifts are entirely due to *s*-CEP contributions. Under that assumption we would have

previously assigned values of $h_2 = -3.5$ kG/ μ_0 , $h_3 = (\pm)1.9$ kG/ μ_0 , and $h_4 = 2.1$ kG/ μ_0 as the shifts for the Fe₃Si alloy system, whereas here we have $h_2 = -0.2$ kG/ μ_0 , $h_3 = -1.3$ kG/ μ_0 , and $h_4 = 0.6$ kG/ μ_0 . Thus, much of the observed shifts come from moment changes, and we see that in order to obtain the h_n values it is necessary to take into account the moment changes as done here.

The h_n values obtained here give quite an odd shape to the s -CEP curve. However, since this polarization arises from both Coulomb exchange and hybridization interactions, the observed shape can easily be obtained by the superposition of these two types of contributions.⁸ We have reexamined the h_n values used previously for the dilute Fe alloys^{3,4} and find that for this system a positive h_3 still appears to be necessary to obtain agreement with the measured spectra of dilute Co and Ni alloys.

E. Hyperfine fields at H_{Si}^0 and H_{Si}^3

The sign of the hff at Si is difficult to measure but there is some evidence²¹ that it is positive. However, this evidence is not conclusive since the applied field used to shift the resonance frequency was not large enough, and the frequencies were not measured accurately enough, to also see if there was also an opposite shift in the Fe A frequency. We shall see if there is any evidence for any particular sign within the model used here. First, we need the hff coupling constant of Si.

The relative behavior of the hff coupling constants of elements in a given row of the Periodic Table can be calculated quite reliably. However, there is less reliability in comparing elements in different rows.

TABLE V. Measured and derived parameters of the Fe₃Si system.

Quantity	Measured	Derived
h_1 (kG/ μ_0)		-12.0
h_2 (kG/ μ_0)		-0.2
h_3 (kG/ μ_0)		-1.3
h_4 (kG/ μ_0)		+0.6
Δ_1 (μ_0)		+0.3
Δ_2 (μ_0)		-0.06
Δ_4 (μ_0)		-0.03
$d\bar{\mu}/dx$ (μ_0 /at. %)	+3.7	+3.7
H_A^0 (kG)	-222	-222
H_B^0 (kG)	-342	-342
H_Σ^D (kG)		-102
H_A^1 (kG)	-52.3	-53.6
H_B^2 (kG)	-7.5	-7.4
H_Σ^3 (kG)		-8
H_A^4 (kG)	+4.2	+4.0

The low- Z elements are especially difficult to know accurately, e.g., the values of Refs. 18 and 19 differ by a factor of 2.0–2.5 near Si. We thus obtain A_{Si}/A_{Fe} as follows. We assume that Al has a small enough atomic volume so that it has no volume misfit contribution. Thus its hff (-62 kG) as a solute in Fe is entirely due to s -CEP. Therefore, $H_{Al} = H_\Sigma^{Fe} A_{Al}/A_{Fe}$ and using $H_\Sigma^{Fe} = -155$ kG we obtain $A_{Al}/A_{Fe} = 0.40$. This agrees fairly well with the calculated ratio 0.49 of Campbell¹⁹ but is in strong disagreement with the ratio 0.92 of Watson and Bennett.²⁰ We thus use the ratio of $A_{Si}/A_{Al} = 1.42$ from Campbell to obtain $A_{Si}/A_{Fe} = 0.57$. The hff coupling constant ratios we use are listed in Table VI. Taking A_{Fe} to be 1.9 MG we find $A_{Si} = 1.1$ MG. The calculated value of H_Σ^D of Eq. (6) is -102 kG. This gives $H_{Si}^0 = 58 + H_V^{Si}$ or $H_V^{Si} = 91$ kG for H_{Si}^0 positive or +17 kG if H_{Si}^0 is negative.

The hff shift at Si due to a 3nn Fe D was measured⁸ to be $[2.5 \pm 1]$ kG or H_Σ^3 of Eq. (9) $\approx [4.4 \pm 2]$ kG. The calculated H_Σ^3 value is -8 kG. The negative sign arises because the first two terms in Eq. (9) dominate. A negative ΔH_{Si}^3 value indicates that H_{Si}^0 is positive.

III. Fe₂^AFe_{1-x}^BT_x^BSi SYSTEMS

The hff values for a number of sites in this system have been measured^{9,10} for $T = V$ and Mn. We now proceed to use the h_n values obtained for the Fe₃Si system and derive values of the solute moment and the moment perturbations due to the element T . We will see that, similar to the moment perturbations found to exist for dilute alloys of Fe,^{3,4} these moment perturbations again resemble RKKY-like oscillations (presumably from the d_i -like electrons). The solute moments also show a very similar behavior to that seen in the dilute Fe alloys.

Here we again consider only the alloys near stoichiometry ($x \approx 0$) in order to maintain additivity

TABLE VI. Hyperfine-field-related quantities used in the analysis.

Quantity	Value
A_{Si}/A_{Al}	1.42
A_{Al}/A_{Fe}	0.40 (expt.)
A_{Si}/A_{Fe}	0.57
A_V/A_{Fe}	0.67
A_{Mn}/A_{Fe}	0.89
A_{Co}/A_{Fe}	1.14
A_{Ni}/A_{Fe}	1.28
A_{Fe}	1.9 MG
H_Σ^{Fe}	-155 \pm 10 kG (expt.)
H_M^{Fe}	-86 \pm 5 kG/ μ_0 (expt.)

of the *s*-CEP contributions and moment perturbations. All the transition elements are small in size and have an effective charge near one, so there are no volume misfit contributions or charge perturbations. We give in Table VII a list of the occupational distribution of the various atoms surrounding a solute *T* atom in an Fe *B* site. As in Sec. II we write the hff values at various sites keeping terms through the 4nn.

A. Hyperfine field at the solute atom *T*

The hff H_T^0 at the solute atom in an Fe *B* site is given by

$$H_T^0 = H_M^T \mu_T + 8h_1^T (\mu_A + \Delta_1^T) + 12h_3^T (\mu_B + \Delta_3^T) + 24h_4^T (\mu_A + \Delta_4^T) \quad (11)$$

where H_M^T is the hff per μ_0 from core polarization and self-polarization by the solute atom itself, and μ_T is the solute-atom moment. The h_n^T values are the *s*-CEP contributions at the solute and are related to those measured in Sec. II at an Fe atom through the hff coupling constants, e.g.,

$$h_n^T = h_n A_T / A_{Fe} \quad (12)$$

The h_n^T values are the moment perturbations caused by the solute atoms and we keep terms through Δ_4^T . The Δ_n^T are expected⁴ to depend on the difference in the number of itinerant *d*-like electrons characteristic of the *T* solute atom compared to the number characteristic of the host. As before, we do not differentiate between the number of *d* electrons of

the various Fe site atoms; we assume their difference is a negligible effect. The H_T^0 fields have been measured to be^{9,10} $(-47.7 - 4) = (-51.7)$ kG for V and $(-259 - 4) = -263$ kG for Mn.

B. First-nearest-neighbor shift for Fe *A* atoms

The Fe *A* atoms which are 1nn to the solute *T* atom in an Fe *B* site will have a hff shift $\delta H_A = H_A^1 - H_A^0$. It can be written from Table VII to be

$$\delta H_A = H_M^{Fc} \Delta_1^T + h_1 (\mu_T - \mu_B) + 3h_1 \Delta_3^T + 3h_2 \Delta_1^T + 3h_2 \Delta_4^T + 3h_3 \Delta_1^T + 6h_3 \Delta_4^T + 6h_4 \Delta_3^T \quad (13)$$

This has been measured by Niculescu *et al.*¹⁰ to be +38 kG for a Mn solute atom and +51 kG for a V solute.

C. Second-nearest-neighbor shift of Si atoms

The Si *D* atoms which are 2nn to the solute *T* atom in an Fe *B* site will have a hff shift $\delta H_{Si}^2 = H_{Si}^2 - H_{Si}^0$. From Table VII δH_{Si}^2 is given by

$$\delta H_{Si}^2 = [h_2 (\mu_T - \mu_B) + 4h_1 \Delta_1^T + 4h_1 \Delta_4^T + 4h_2 \Delta_3^T + 4h_4 \Delta_1^T + 8h_4 \Delta_4^T] A_{Si} / A_{Fe} \quad (14)$$

The assumption has been made that an H_V^{Si} term is the same whether or not the Si *D* atom has a 2nn *T* atom. The value of δH_{Si}^2 has been measured²² to be |2.4| kG for Mn and |2.8| kG for V. A + sign applies if H_{Si}^0 is positive.

TABLE VII. Occupational distribution for various atoms which are *n*th neighbor to a *T* atom in an Fe *B* site.

1nn	Shell with respect to <i>TB</i>	2nn	Shell with respect to <i>TB</i>	3nn	Shell with respect to <i>TB</i>	4nn	Shell with respect to <i>TB</i>
Fe <i>A</i> which is 1nn to <i>TB</i>							
<i>TD</i>	1nn	3 Fe <i>A</i>	1nn	3 Fe <i>A</i>	1nn	3 Si <i>D</i>	2nn
3 Si <i>D</i>	2nn	3 Fe <i>A</i>	4nn	6 Fe <i>A</i>	4nn	6 Fe <i>B</i>	3nn
3 Fe <i>B</i>	3nn			3 Fe <i>A</i>	7nn	9 Si <i>D</i>	>4nn
1 Si <i>D</i>	5nn					6 Fe <i>B</i>	>4nn
Si <i>D</i> which is 2nn to <i>TB</i>							
4 Fe <i>A</i>	1nn	<i>TB</i>	2nn	4 Si <i>D</i>	2nn	4 Fe <i>A</i>	1nn
4 Fe <i>A</i>	4nn	4 Fe <i>B</i>	3nn	4 Si <i>D</i>	5nn	8 Fe <i>A</i>	4nn
		1 Fe <i>B</i>	6nn	4 Si <i>D</i>	8nn	12 Fe <i>A</i>	>4nn
<i>TB</i> or Fe <i>B</i> which is 3nn to <i>TB</i>							
2 Fe <i>A</i>	1nn	2 Si <i>D</i>	2nn	<i>TB</i>	3nn	4 Fe <i>A</i>	1nn
4 Fe <i>A</i>	4nn	2 Si <i>D</i>	5nn	4 Fe <i>B</i>	3nn	6 Fe <i>A</i>	4nn
2 Fe <i>A</i>	7nn	2 Si <i>D</i>	8nn	7 Fe <i>B</i>	>4nn	14 Fe <i>A</i>	>4nn

D. Third-nearest-neighbor shift of T atoms

A T solute atom, which is 3nn to another T atom, will not have the same moment perturbation as an Fe atom in the same shell. Thus, we denote the moment perturbations at another T solute atoms by δ_n^T . We expect the δ_n^T to be near zero since both T atoms have similar numbers of d_i electrons. From Table VII we see that this hff shift $\delta H_T^3 = H_T^3 - H_T^0$ is

$$\begin{aligned} \delta H_T^3 = & H_M^T \delta_3^T + h_3^T (\mu_T + \delta_3^T - \mu_B - \Delta_3^T) + 2h_1^T \Delta_1^T \\ & + 4h_1^T \Delta_4^T + 4h_3^T \Delta_3^T + 4h_4^T \Delta_1^T + 6h_4^T \Delta_4^T . \end{aligned} \quad (15)$$

This shift has been measured^{9,10} to be +5.7 kG for Mn and +4.7 kG for V.

E. Third-nearest-neighbor shift for Fe B atoms

For Fe B atoms which are 3nn to the T solute atoms the hff shift $\delta H_B^3 = H_B^3 - H_B^0$ is given by

$$\begin{aligned} \delta H_B^3 = & H_M^{Fc} \Delta_3^T + h_3 (\mu_T - \mu_B) + 2h_1 \Delta_1^T + 4h_1 \Delta_4^T \\ & + 4h_3 \Delta_3^T + 4h_4 \Delta_1^T + 6h_4 \Delta_4^T . \end{aligned} \quad (16)$$

This shift was measured^{9,10} to be +9.4 kG for dilute alloys of Mn. Its value in V is difficult to determine with reliability because the V resonance falls close to the Fe B line and is of much greater intensity.

It is sometimes assumed¹⁰ that δH_T^3 and δH_B^3 scale simply as the hff coupling constants. We see from Eqs. (15) and (16) that they are related by

$$\delta H_B^3 = \frac{\delta H_T^3 A_{Fe}}{A_T} + \Delta_3^T (H_M^{Fc} + h_3) - \delta_3^T \left[\frac{H_M^T A_{Fe}}{A_T} + h_3 \right] . \quad (17)$$

Thus, there should be no simple scaling unless Δ_3^T and δ_3^T are zero. We expect δ_3^T to be nearly zero but in general Δ_3^T will not be zero. Evaluating the known quantities in Eq. (17) we find

$$\delta_3^{Mn} = 0.029 + 0.85 \Delta_3^{Mn} . \quad (18)$$

We will see below that δ_3^{Mn} is essentially zero as expected, but $\Delta_3^{Mn} \neq 0$.

TABLE VIII. Measured quantities for Mn and V solute atoms (all hff values in kG) (Refs. 9–11).

	$\frac{d\mu}{dx}$ (μ_0/atom)	H_T^0	δH_A^1	δH_B^3	δH_T^3	$\delta H_{S_i}^2$
Mn	-2.66	-263	38	9.4	5.7	(\pm)2.4
V	-4.84	(-) 51.7	51	...	4.7	(\pm)2.8

F. Saturation magnetization

The slope of the saturation magnetization as a function of solute concentration gives the following equation relating the solute moment and moment perturbations:

$$\frac{d\mu}{dx} = \mu_T - \mu_B + 8\Delta_1^T + 12\Delta_3^T + 24\Delta_4^T . \quad (19)$$

For this analysis we want the initial slope. We use values from Ref. 11 which are listed in Table VIII.

G. Evaluation of μ_T and Δ_n^T for Mn and V

In order to evaluate the μ_T and Δ_n^T values we need the H_M^T values, ($H_M = H_{cp} + H_s$). These are obtained as follows: A rather reliable value for H_{cp}^{Fc} can be obtained from band calculations. The results of several band calculations (see Table V of Ref. 23) give $H_{cp}^{Fc} \approx -160$ kG/ μ_0 . As discussed earlier, H_M^{Fc} is known quite accurately from experiment (-86 kG/ μ_0). Thus, the value of H_s^{Fc} is 74 kG/ μ_0 . The other H_{cp}^T values are obtained from the calculated variation of this quantity for the neutral Fe series and the H_s^T values are found from the value of H_s^{Fc} by $H_s^T = H_s^{Fc} A_T / A_{Fe}$. The H_M^T values are then found from their sums. All values involved are listed in Table IX. The results are quite insensitive to reasonable variations of H_{cp}^{Fc} . We now evaluate the μ_T and Δ_n^T values using the equations derived for this system.

1. Mn

For Mn we have four measured quantities, $d\mu/dx$, H_T^0 , δH_A^1 , and δH_B^3 which contain only μ_{Mn} , Δ_1 , Δ_3 , and Δ_4 as unknowns. These are listed in Table VIII. A fifth measured quantity $\delta H_{S_i}^2$ is less reliable since it contains the ratio A_{S_i}/A_{Fe} . A sixth measured quantity δH_T^3 contains another parameter δ_3^{Mn} which we expect to be zero, if the moment perturbations are due to the proposed mechanism of d_i polarization. We first evaluate the four unknown moments from the known measured quantities. The results are listed in Table X. Using Eq. (18) to calculate δ_3^{Mn} we find that it is indeed zero within the accuracy of the measure-

TABLE IX. Hyperfine-field-related quantities used in the analysis.

T	H_{cp}^T (kG/ μ_0)	H_s^T (kG/ μ_0)	H_M^T (kG/ μ_0)
V	-145	50	-95
Mn	-156	66	-90
Fe	-160	74	-86
Co	-165	84	-81
Ni	-169	95	-74

ments, i.e., $\delta_3^{\text{Mn}} = -0.004$ as compared to the larger Δ_3^{Mn} value of -0.039 . Thus, the fact that $\delta H_D^3 \neq \delta H_T^3$ indicates that there is a 3nn moment perturbation from the Mn solute atom. Alternately, if δ_3^{Mn} is assumed to be zero, the Mn system is overdetermined, and the value of δH_{Mn}^3 is found to be in excellent agreement with the moments obtained from the other measured quantities. The value of δH_{Si}^3 calculated from Eq. (14) is found to be $+7.4$ kG. The measured value²² of δH_{Si}^3 is $+2.4$ kG for a positive value of H_{Si}^0 , so again H_{Si}^0 seems to be positive.

2. V

As seen in Table VIII there are five measured quantities for V. The V resonance is close to the H_B^0 resonance and much more intense, so the δH_B^3 value is not reliably established. Thus, we have not used it in the analysis, but instead have calculated it from the Δ_n values determined by using δH_V^3 (with $\delta_3^{\text{V}} = 0$) along with $d\bar{\mu}/dx$, H_V^0 and δH_A^3 . We give in Table X the resulting moment perturbations determined by this procedure. The value of δH_{Si}^3 calculated with the derived μ_V and Δ_n is $+3.6$ kG, in good agreement with the measured value $|2.8|$ kG. Again the sign indicates that H_{Si}^0 is positive. The V solute atom is seen to be aligned antiferromagnetically as in the case of the dilute Fe alloys. It is found to have a value of $-0.3 \mu_0$ as compared to $-0.2 \mu_0$ in the dilute Fe alloys. This corresponds to the hff at the V atom being composed of $+40$ kG from the moment on V and -92 kG from the s -CEP contribution. This is a very different result from that of Niculescu *et al.*¹⁰ where a nearest-neighbor-only solution was used, and it was concluded that μ_V was essentially zero and all the hff at V was all due to s -CEP. We show the moment perturbations for Mn and V in Fig. 2.

TABLE X. Derived moments and moment perturbations for Mn and V (all moments in μ_0 and hff values in kG).

	This work	Niculescu <i>et al.</i> ¹⁰	Pure Fe
μ_{Mn}	1.7	2.2	1.0
Δ_1^{Mn}	-0.32	-0.34	-0.06
Δ_3^{Mn}	-0.039		$\Delta_2 = -0.11$
Δ_4^{Mn}	+0.044		$\Delta_3 = \Delta_4 = 0.016$
δ_3^{Mn}	-0.003		
μ_V	-0.28	-0.02	-0.2
Δ_1^{V}	-0.16	-0.34	+0.17
Δ_3^{V}	-0.14		$\Delta_2 = -0.35$
Δ_4^{V}	+0.036		$\Delta_3 = \Delta_4 = 0.01$
δH_{Si}^3 (calc.)	+3.6		
δH_B^3 (calc.)	18.5		

IV. $\text{Fe}_{2-x}^{\text{A,C}}\text{Fe}^{\text{B}}\text{T}_V^{\text{A}}\text{Si}$ SYSTEMS

The transition elements below and to the right of Fe in the Periodic Table have been shown to go into Fe A or C sites. We list the occupational distributions for the surrounding sites in Table XI. We consider data for $T = \text{Co}$ or Ni. Unfortunately, in these alloys, very few, if any, satellites have been seen; mainly, only broadening of the spectra occurs. We give the expressions for the hff shifts anyway, so we can estimate their sizes.

A. hff at solute atom T

The hff H_T^0 at the solute atom in site A is given by

$$H_T^0 = H_M^T \mu_T + 4h_1^T (\mu_B + \Delta_1^T) + 6h_2^T (\mu_A + \Delta_2^T) + 12h_3^T (\mu_A + \Delta_3^T) + 12h_4^T (\mu_B + \Delta_4^T) \quad (20)$$

These values have been measured to be⁹ -197 kG for Co and -164 kG for Ni. These values include -4 kG for the Lorentz term $(\frac{4}{3}\pi)M_s$.

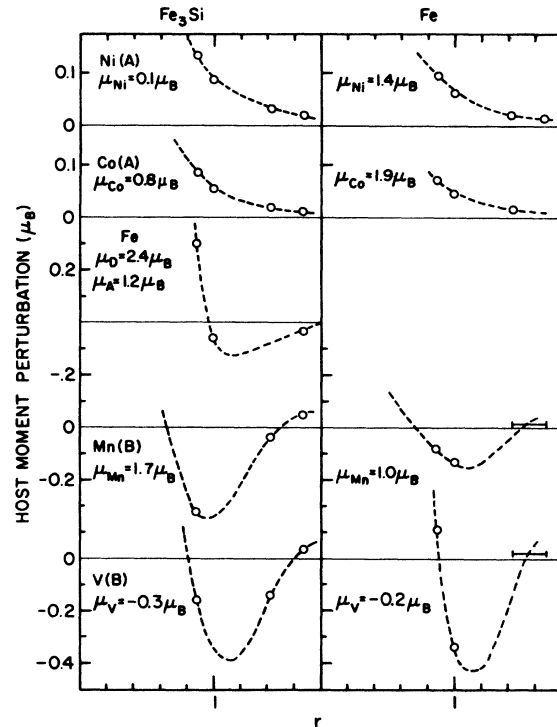


FIG. 2. Host moment perturbations surrounding transition-metal solute atoms as a function of distance from a solute atom (in units of the 2nn distance). The left-hand side shows the moment perturbations in a Fe_3Si host while the right-hand side shows them in an Fe host. The Ni and Co are on Fe A sites, the Mn and V are on Fe B sites in Fe_3Si .

TABLE XI. Occupational distribution for various atoms which are n th neighbor to a T atom in an Fe A or C site.

1nn	Shell with respect to TA	2nn	Shell with respect to TA	3nn	Shell with respect to TA	4nn	Shell with respect to TA
Si or Fe D atom which is 1nn to TA							
TA		3 Fe B , Si D	1nn	3 Si D , Fe B	1nn	3 Fe A	2nn
3 Fe A	2nn	3 Fe B , Si D	4nn	6 Si D , Fe B	4nn	6 Fe A	3nn
2 Fe A	3nn			3 Si D , Fe B	7nn	15 Fe A	4nn
1 Fe A	5nn						
T or Fe A atom which is 2nn to TA							
2 Fe B	1nn	TA	2nn	4 Fe A	2nn	2 Fe B	1nn
2 Si D	1nn	4 Fe A	3nn	4 Fe A	5nn	2 Si D	1nn
2 Fe B	4nn	1 Fe A	6nn	4 Fe A	8nn	4 Fe B	4nn
2 Si D	4nn					4 Si D	4nn
						6 Fe B	>4nn
						6 Si D	>4nn
T or Fe A atom which is 3nn to TA							
1 Fe B	1nn	2 Fe A	2nn	TA	3nn	2 Fe B	1nn
1 Si D	1nn	2 Fe A	5nn	4 Fe A	3nn	2 Si D	1nn
2 Fe B	4nn	2 Fe A	8nn	7 Fe A	>4nn	3 Fe B	4nn
2 Si D	4nn					3 Si D	4nn
1 Fe B	7nn					7 Fe B	>4nn
1 Si D	7nn					7 Si D	>4nn

B. First-nearest-neighbor shift at Si D or Fe B atoms

From Table XI we can write the hff shifts $\delta H_{Si}^1 = H_{Si}^1 - H_{Si}^0$ and $\delta H_B^1 = H_B^1 - H_B^0$. We have

$$\delta H_{Si}^1 = [h_1(\mu_T - \mu_A) + 3h_1\Delta_2^T + 3h_1\Delta_3^T + 3h_2\Delta_1^T + 3h_2\Delta_4^T + 3h_4\Delta_2^T + 6h_4\Delta_3^T]A_{Si}/A_{Fe} \quad (21)$$

$$\delta H_B^1 = H_M^{Fc}\Delta_1^T + h_1(\mu_T - \mu_A) + 3h_1\Delta_2^T + 3h_1\Delta_3^T + 3h_3\Delta_1^T + 6h_3\Delta_4^T + 3h_4\Delta_2^T + 6h_4\Delta_3^T \quad (22)$$

A shift of δH_{Si}^1 of about (+)2 kG has been measured.²² No clear satellite is seen on the Fe B line.

C. Second-nearest-neighbor shift at T atom

The hff shift at a T atom which is 2nn to another T atom is given by $\delta H_T^2 = H_T^2 - H_A^0$,

$$\delta H_T^2 = H_M^T\delta_2^T + h_2^T(\mu_T + \delta_2^T - \mu_A - \Delta_2^T) + 2h_1^T\Delta_1^T + 2h_1^T\Delta_4^T + 4h_2^T\Delta_3^T + 4h_3^T\Delta_2^T + 2h_4^T\Delta_1^T + 4h_4^T\Delta_4^T \quad (23)$$

This has been tentatively measured⁹ to be -2.5 kG for Co.

D. Third-nearest-neighbor shift at T atom

The hff shift at a T atom which is 3nn to another TA atom is given by $\delta H_T^3 = H_T^3 - H_A^0$,

$$\delta H_T^3 = H_M^T\delta_3^T + h_3^T(\mu_T + \delta_3^T - \mu_A - \Delta_3^T) + h_1^T\Delta_1^T + 2h_1^T\Delta_4^T + 2h_2^T\Delta_2^T + 4h_3^T\Delta_3^T + 2h_4^T\Delta_1^T + 3h_4^T\Delta_4^T \quad (24)$$

These have been tentatively determined to be +1.6 kG for Co and -4.0 kG for Ni.

E. Saturation magnetization

The initial slopes of the saturation magnetization curve for Co and Ni solute atoms are only roughly determined.¹¹ We know from dilute Fe alloy behavior that the slope starts out positive and bends over to become negative at higher concentrations. This is also seen to be the case for Fe₃Si as a host, but the data are very sparse. Thus, the values of $d\mu/dx$ may be quite inaccurate. The initial slopes are taken to be +0.50 μ_0 / (Co atom) and +0.60 μ_0 / (Ni atom) from the data of Ref. 11. From Table III we see that the initial slope for T atoms in Fe A sites is given by

$$\frac{d\mu}{dx} = \mu_T - \mu_A + 4\Delta_1 + 6\Delta_2 + 12\Delta_3 + 12\Delta_4 \quad (25)$$

The positive values of $d\mu/dx$ indicate that the moment perturbations are predominantly positive, as was the case for dilute alloys of Co and Ni in an Fe host.

F. Evaluation of μ_T and Δ_n^T values

Only H_T^0 is additionally identified⁹ in alloys with Co and Ni solute atoms. There is also some broadening of the lines due to other shifts. Thus, the outstanding feature of these solute atoms is that the shifts, due to nearby Co and Ni atoms, are small. Therefore, we investigate the moment perturbations under two different types of distributions: (a) Assuming only a 1nn perturbation, i.e., $\Delta_1 \neq 0$, $\Delta_2 = \Delta_3 = \Delta_4 = 0$, and (b) a widespread distribution similar to that seen in the dilute binary alloys where Δ_n varies as r_n^{-3} . For both cases we assume $\delta_n^T = 0$, which should be a good assumption. From previous evaluation of the dilute alloys of Co and Ni in Fe it appeared that these solutes have some orbital contribution. To include this possibility we therefore evaluate two cases, one with $H_{orb} = 0$ and the other for $H_{orb} = 20$ kG for Co and 10 kG for Ni.

1. Co

We use only $d\mu/dx$ and H_{Co}^0 in the evaluations. With only $\Delta_1 \neq 0$ we obtain $\mu_{Co} = 0.6-0.9 \mu_B$ and $\Delta_1 = 0.28-0.21 \mu_B$. Some of the hff shifts obtained in this approximation are large, they are listed in Table XII. For the r_n^{-3} moment perturbations we obtain $\mu_{Co} = 0.7-1.0 \mu_0$ and $\Delta_1 = 0.08-0.06 \mu_0$. The hff shifts obtained with this distribution are all quite small, they are listed in Table XII. Thus, the experimentally observed small shifts indicate that the moment perturbations are widespread as was also the case for the dilute binary alloys of Co in Fe. The calculated values of δH_{Si}^0 and δH_{Co}^2 agree well with the tentatively measured values.

2. Ni

Again we use only $d\mu/dx$ and H_{Ni}^0 in the evaluation. For the 1nn-only perturbation we find the unlikely solution $\mu_{Ni} = -0.25\mu_0$ to $-0.08 \mu_0$ and $\Delta_1 = 0.5 \mu_0$. For the moment perturbations varying as r_n^{-3} we obtain the more reasonable values of $\mu_{Ni} = 0.05-0.2 \mu_0$ and $\Delta_1 \approx 0.14 \mu_0$. The hff shifts obtained in both approximations are given in Table XII. Again the r_n^{-3} perturbations give small hff shifts, whereas the 1nn-only perturbation gives large shifts. Since only small broadenings occur in the Ni spectra, the moment perturbations surrounding a Ni atom appear to be widespread. As can be seen from Table XII, the results are not very sensitive to a reasonable amount of orbital contribution. We show the r_n^{-3} moment perturbation surrounding Co and Ni solutes in Fig. 2.

V. SUMMARY AND CONCLUSIONS

Using the measured hff values and shifts obtained when Fe atoms are substituted into Si *D* sites, we have derived the hff shifts and moment perturbations in the Fe₃Si system near stoichiometry. We then assume that these derived hff shifts are inherent to the s-CEP of the Fe₃Si system and use them to obtain the solute moment and moment perturbations resulting from substituting Mn or V into an Fe *B* site or Co or Ni into an Fe *A* site. The resulting moment perturbations are shown in Fig. 2.

We find the following results:

(a) Considering the uncertainty in A_{Si} the calculated and measured shifts for the Si sites are in satisfactory agreement. They support the sign of the hff at Si being positive.

(b) The moment values of the solutes in Fe₃Si vary in the manner expected from comparison with their moments in Fe (see Fig. 2). The Fe *B* site has a moment slightly larger ($2.4 \mu_B$) than that of pure Fe; both Mn and V which go into Fe *B* sites also appear to have

TABLE XII. Calculated moments and hff shifts for Co and Ni in Fe *A* sites (all hff values in kG and moments in μ_0).

	1nn approximation				r_n^{-3} approximation			
	Co		Ni		Co		Ni	
	$H_{orb} = 0$	$H_{orb} = 20$	$H_{orb} = 0$	$H_{orb} = 10$	$H_{orb} = 0$	$H_{orb} = 20$	$H_{orb} = 0$	$H_{orb} = 10$
μ_T	0.6	0.9	-0.25	-0.08	0.7	1.0	0.05	0.2
Δ_1^T	0.28	0.21	0.52	0.47	0.08	0.06	0.14	0.13
δH_{Si}^1	4.2	2.2	9.8	8.7	2.0	0.6	5.5	4.7
δH_B^1	-17.6	-14.7	-22.6	-27.0	-3.8	-4.4	-1.5	-3.6
δH_T^2	-6.2	-5.6	-14.7	-12.0	-2.6	-1.9	-5.0	-4.6
δH_T^3	-2.2	-2.1	-4.7	-3.9	-0.7	-0.7	-0.8	-0.8

slightly larger moments than they do in Fe host. Due to having only four nearest-neighbor Fe atoms, the Fe *A* atoms have a much smaller moment ($1.2 \mu_0$) than that of pure Fe; both Co and Ni which go into Fe *A* sites also have much smaller moments than they do in an Fe host.

(c) The moment perturbations show the same general behavior as is seen for the dilute binary Fe alloys, also shown in Fig. 2. The first node moves in, as the *3d* transition series is crossed from right to left, due to the increasing number of *d*_i electrons

contributed by the solute atom. Thus apparently the electronic bond structure of Fe₃Si is similar to that of pure Fe resulting in a similar polarization behavior of the *d*_i electrons. It has previously been proposed that it is this polarization which is responsible for the alignment of the atomic moment in *3d* ferromagnets. Since the Fe₃Si lattice is closely related to Heusler alloys, we suggest that their magnetic behavior is also mainly determined by the alignment of the localized spin through the polarized *d*_i-like, rather than *s*-like, conduction electrons.

-
- ¹M. B. Stearns, *J. Magn. Magn. Mater.* **5**, 167 (1977).
²P. M. Tedrow and R. Meservey, *Phys. Rev. Lett.* **26**, 191 (1971); *Phys. Rev. B* **7**, 318 (1973); R. Meservey, D. Paraskevopoulos, and P. M. Tedrow, *Phys. Rev. Lett.* **37**, 858 (1976).
³M. B. Stearns, *Phys. Rev. B* **9**, 2311 (1974).
⁴M. B. Stearns, *Phys. Rev. B* **13**, 1183 (1976).
⁵M. B. Stearns, *Phys. Rev.* **129**, 1136 (1963).
⁶A. Paolette and L. Passari, *Nuovo Cimento* **32**, 25 (1964).
⁷J. I. Budnick, S. Skalski, and T. J. Burch, *J. Appl. Phys.* **38**, 1137 (1967).
⁸M. B. Stearns, *Phys. Rev. B* **4**, 4069 (1971); **4**, 4081 (1971).
⁹T. J. Burch, T. Litrenta, and J. I. Budnick, *Phys. Rev. Lett.* **33**, 421 (1974); T. Litrenta, Ph.D. thesis (Fordham University, 1975) (unpublished).
¹⁰V. Niculescu, K. Raj, T. J. Burch, and J. I. Budnick, *Phys. Rev. B* **13**, 3167 (1967); V. Niculescu, K. Raj, J. I. Budnick, T. J. Burch, W. A. Hines, and A. H. Menotti, *ibid.* **14**, 4160 (1976).
¹¹W. A. Hines, A. H. Menotti, J. I. Budnick, T. J. Burch, T. Litrenta, V. Niculescu, and K. Raj, *Phys. Rev. B* **13**, 4060 (1976). The values of $d\bar{\mu}/dx$ for binary Fe alloys given in Table II are incorrect since at. % was used instead of wt. %.
¹²M. B. Stearns, *Phys. Rev.* **147**, 439 (1966); *Phys. Rev. B* **8**, 4383 (1973).
¹³M. B. Stearns, *Phys. Lett. A* **34**, 146 (1971); *Phys. Rev. B* **13**, 4180 (1976).
¹⁴R. E. Watson and A. J. Freeman, in *Hyperfine Interactions*, edited by A. J. Freeman and R. B. Frankel (Academic, New York, 1967); D. A. Shirley, *Phys. Lett. A* **25**, 129 (1967).
¹⁵A. Blandin and I. A. Campbell, *Phys. Rev. Lett.* **31**, 51 (1973); I. A. Campbell and A. Blandin, *J. Magn. Magn. Mater.* **1**, 1 (1975).
¹⁶M. B. Stearns, *Phys. Rev. B* **12**, 1626 (1975).
¹⁷M. Kontani and J. Itoh, *J. Phys. Soc. Jpn.* **22**, 345 (1967).
¹⁸D. A. Shirley and G. A. Westerbarger, *Phys. Rev.* **138**, A170 (1965); D. A. Shirley, S. S. Rosenblum, and E. Matthias, *ibid.* **170**, 363 (1968).
¹⁹I. A. Campbell, *J. Phys. C* **2**, 1338 (1969).
²⁰R. E. Watson and L. H. Bennett, *Phys. Rev. B* **15**, 502 (1977).
²¹K. Kumagai, K. Asayama and I. A. Campbell, *J. Phys. Soc. Jpn.* **37**, 1460 (1974).
²²K. Raj (private communication).
²³K. J. Duff and T. P. Das, *Phys. Rev. B* **3**, 2294 (1971).